Reaction $\pi^+ + d \rightarrow p + p$ at 20 to 65 MeV

B. G. Ritchie, R. D. Edge, D. J. Malbrough, and B. M. Preedom
Department of Physics and Astronomy, University of South Carolina, Columbia, South Carolina 29208

F. E. Bertrand, E. E. Gross, F. E. Obenshain, and J. R. Wu
Oak Ridge National Laboratory, Oak Ridge, Tennessee 37830

M. Blecher and K. Gotow
Department of Physics, Virginia Polytechnic Institute and State University, Blacksburg, Virginia 24061

R. L. Burman, R. Carlini, M. E. Hamm, and M. J. Leitch
Los Alamos Scientific Laboratory, Los Alamos, New Mexico 82740

M. A. Moinester
Department of Physics and Astronomy, Tel Aviv University, Ramat-Aviv, Israel
(Received 23 February 1981)

Angular distributions for the reaction $\pi^+ + d \rightarrow p + p$ have been measured for pion laboratory energies ranging from 20 to 65 MeV. Uncertainties in the total cross sections were less than 6% at all energies studied. The angle integrated cross sections were determined to be 4.31 ± 0.18, 4.84 ± 0.20, 4.26 ± 0.16, 5.19 ± 0.21, 5.30 ± 0.25, 5.20 ± 0.28, and 7.40 ± 0.30 mb for pion laboratory energies of 20, 25, 30, 35, 40, 45, and 65 MeV, respectively. These values confirmed the general trend observed for the total reaction cross section at energies below resonance. The angular distributions and integrated cross sections are compared with recent microscopic calculations. Though qualitative agreement is evident between the models used to describe the process and experimental results, quantitative agreement is still lacking.

[NUCLEAR REACTIONS $d(\pi^+,p)p$, $E = 20, 25, 30, 35, 40, 45, 65$ MeV; measured $d\sigma/d\Omega$, deduced total cross section for each energy; obtained fits to $d\sigma/d\Omega$ with polynomials linear and quadratic in $\cos^2\theta$; compared with microscopic calculations for the reaction.]

I. INTRODUCTION

The reaction $\pi^+ + d \rightarrow p + p$ represents the simplest pion annihilation process which occurs in nature. Hence, the reaction has been of great interest in studies of pion-nucleon, nucleon-nucleon, and pion-nucleus interactions. It has also been suggested that the reaction may be used to probe angular momentum components of the deuteron ground state wave function and to study theories of detailed balance. As a consequence of these diverse and fundamental phenomena, the reaction has been intensively studied for nearly three decades, as evidenced in a recent review article.[1]

Accurate measurements of the energy dependences of the reaction angular distribution and total cross section are of particular importance in understanding the mechanisms associated with this reaction. As experimental technologies and techniques have improved, more precise determinations of the integral and differential cross sections have been made at many energies. Though the energy dependence of these quantities has been well established above the pronounced resonance at a pion laboratory energy of approximately 150 MeV, there remain significant discrepancies below resonance for the integrated cross section and many experimental values possess large uncertainties. The purpose of this experiment was to measure total and differential cross sections for the reaction at pion laboratory energies of 20, 25, 30, 35, 40, 45, and 65 MeV to further define the trends of the total and differential cross sections in the below resonance region.

II. EXPERIMENTAL PROCEDURE

The design of this experiment was similar to that used in a previous study of the reaction.[2] The

detection system utilized the back-to-back emission of protons following pion absorption to furnish an unambiguous reaction signature. For completeness, we furnish here a review of the detection system used in our previous experiment and detail the experimental procedures used in this study.

The experiment was performed at the Clinton P. Anderson Meson Physics Facility (LAMPF) low energy pion channel. The target was a solid CD_2 disk of areal density 0.4321 ± 0.0007 g/cm^2. A radiographic assay of the target ascertained its hydrogen constituents to be 98.31% deuterium and 1.69% hydrogen, with variations of much less than 1% in the areal density across the disk.

Data were taken in cycles of six runs at each energy. Each run consisted of observations at four angles, retaining a common angle between runs in a cycle. The common angle permitted relative normalization between data runs within each cycle. The CD_2 target was used in three runs of each cycle, while a CH_2 target of areal density 0.3777 ± 0.0006 g/cm^2 was used for background measurements in the remaining three runs in each cycle.

The detector array consisted of four pairs of plastic scintillator telescopes made of NE102. Each pair consisted of one dE/dx-E telescope and one large solid angle conjugate detector. The detectors in each pair were positioned directly opposite each other in the center-of-mass frame. The dE/dx counters were disks of plastic scintillator material 1.905 ± 0.005 cm in diameter and 0.492 cm thick.

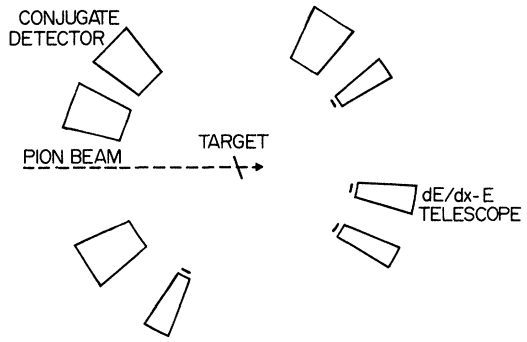

FIG. 1. Typical detector configuration used in this experiment.

Each E telescope was a truncated cone of the scintillator material, with the smaller end physically, though not optically, mated to a dE/dx counter. The large solid angle conjugate detectors were wedge-shaped blocks of scintillator material, with the smallest side of the wedge facing the target. The smallest face on each conjugate detector was approximately 8.9×12.7 cm, the larger dimension being oriented perpendicular to the plane formed by the detectors. Due to its smaller size, the dE/dx counter determined the solid angle for each detector pair. The distance from the target to the dE/dx counter in each pair was 25.400 ± 0.013 cm, yielding a solid angle of 4.466 ± 0.013 msr. A typical detector configuration is shown in Fig. 1.

The conjugate counter solid angle had to be great enough in each detector pair to detect protons from

TABLE I. Absolute differential cross sections determined in this experiment.

Energy (MeV)	Data run	Lab angle (deg)	$d\sigma/d\Omega$ (mb/sr)	relative error (%)
20	I	16.5	1.210	1.91
		32.8	1.034	2.01
		38.3	0.912	2.16
		115.3	0.547	3.09
	II	21.9	1.190	2.38
		43.6	0.850	1.60
		49.0	0.753	3.10
	III	43.6	0.845	2.29
		64.9	0.563	2.89
		85.6	0.404	3.53
		115.3	0.547	3.18
25	I	16.6	1.393	1.96
		33.2	1.159	1.94
		38.6	1.034	2.08

TABLE I. *(Continued).*

		115.9	0.568	3.14
	II	22.2	1.298	2.40
		27.7	1.234	2.51
		44.1	0.981	2.79
		49.5	0.808	3.09
	III	44.1	0.889	2.44
		65.5	0.557	3.19
		86.2	0.395	3.97
		111.1	0.572	3.51
30	I	16.8	1.286	3.09
		33.4	1.103	3.31
		38.9	0.992	3.54
		116.4	0.467	5.84
	II	22.4	1.277	2.16
		27.9	1.200	2.27
		44.4	0.828	2.67
		49.9	0.812	2.78
	III	44.4	0.826	1.75
		65.9	0.514	2.29
		86.7	0.331	2.94
		111.6	0.450	2.66
35	I	33.7	1.277	1.87
		39.2	1.191	1.94
		116.9	0.658	3.02
	II	22.5	1.452	2.47
		28.1	1.456	2.51
		44.8	0.999	3.07
		50.2	0.953	3.19
	III	44.8	0.998	1.87
		66.4	0.612	2.57
		87.2	0.421	3.18
		112.1	0.585	2.87
40	I	33.9	1.301	1.67
		39.5	1.189	1.78
		117.3	0.623	2.82
	II	28.3	1.436	1.99
		45.1	1.023	2.39
		50.6	0.941	2.50
	III	45.1	1.046	1.61
		66.8	0.629	2.10
		87.7	0.419	2.81
		112.5	0.634	2.42
45	I	17.2	1.452	3.46
		34.2	1.321	3.24
		39.8	1.103	2.02
		117.7	0.718	2.92
	II	22.8	1.523	2.07
		45.3	1.056	1.59
		50.9	0.935	2.76
	III	45.3	1.056	1.68
		67.2	0.590	2.28
		88.1	0.405	2.93

TABLE I. *(Continued).*

		112.9	0.552	2.69
65	I	17.5	2.383	3.20
		34.9	1.937	3.60
		40.6	1.780	3.76
		119.1	0.882	6.10
	II	23.4	2.153	2.02
		29.1	2.012	2.16
		51.9	1.290	3.00
	III	68.5	0.788	2.17
		89.6	0.516	2.85
		114.3	0.832	2.37

the reaction which had undergone multiple Coulomb scattering and were paired with protons registering in the dE/dx detectors. Calculations verified that the size of the conjugate counters was more than sufficient. Dead time corrections for all detector pairs were measured to be negligible. It was also important to correct the observed proton flux in the E and conjugate detectors for losses due to reactions undergone by the protons in the scintillation material of the telescopes. These corrections were based on measured counter responses reported in a previous publication.[3]

The use of a CD_2 target resulted in some background under the reaction $2p$ peak from $^{12}C(\pi^+,2N)X$ reactions. The background for the ^{12}C content of the CD_2 target was determined with the CH_2 target data runs, subtracting the CH_2 spectrum from the CD_2 spectrum after proper normalization for beam flux and target density. It was found that such contamination necessitated only a very small correction to the CD_2 spectra, generally less than 3%.

Relative monitoring of the pion flux was accomplished by detecting muons from the decay of beam pions with a scintillation counter situated above the pion beam. This counter was at an angle well within the Jacobian peak angle for the muon distribution. Counting rates in this telescope were approximately 1000 per sec during data runs and 10 per sec during monitor calibration runs. This relative monitor was fixed in position throughout each data taking cycle. Absolute normalization of this relative monitor for beam intensity was accomplished at each energy by removing the CD_2 target and placing a pair of plastic scintillators (2.54 cm thick) into the reduced intensity pion beam. The scintillator pair provided dE/dx particle identification and thus permitted the determination of the absolute pion flux versus the decay muon flux in the relative monitor during the calibration runs. Reaction losses were taken into account for the in-beam scintillator pair in determining absolute pion flux.

III. EXPERIMENTAL RESULTS AND DISCUSSION

The differential cross section at each angle and energy was determined from the relation

$$\left.\frac{d\sigma}{d\Omega}\right|_{\text{c.m.}} = \frac{N_p}{N_\pi}\frac{\cos\gamma}{\bar{n}\,d\Omega_{\text{lab}}}J(E,\theta)\ , \tag{1}$$

where for each energy E and laboratory angle θ:

N_p represents proton pairs in the reaction peak (corrected for background and absorption); N_π represents the incident pion flux during data taking; $d\Omega_{\text{lab}}$ represents the laboratory solid angle; $\bar{n}$ represents the areal density of the CD_2 target; γ represents the angle between the CD_2 target and the pion beam; and $J(E,\theta)$ represents the laboratory to center-of-mass frame Jacobian.

The absolute differential cross sections and uncertainties determined in this experiment are presented in Table I, and the angular distributions are shown in Fig. 2. The accuracy of the relative normalizations was verified by the common angles.

Fits were made to the data in Table I using the polynomial forms

$$\left.\frac{d\sigma}{d\Omega}\right|_{\text{c.m.}} = C_0 + C_2\cos^2\theta_{\text{c.m.}}\ , \tag{2a}$$

$$\left.\frac{d\sigma}{d\Omega}\right|_{\text{c.m.}} = C_0 + C_2\cos^2\theta_{\text{c.m.}} + C_4\cos^4\theta_{\text{c.m.}} \tag{2b}$$

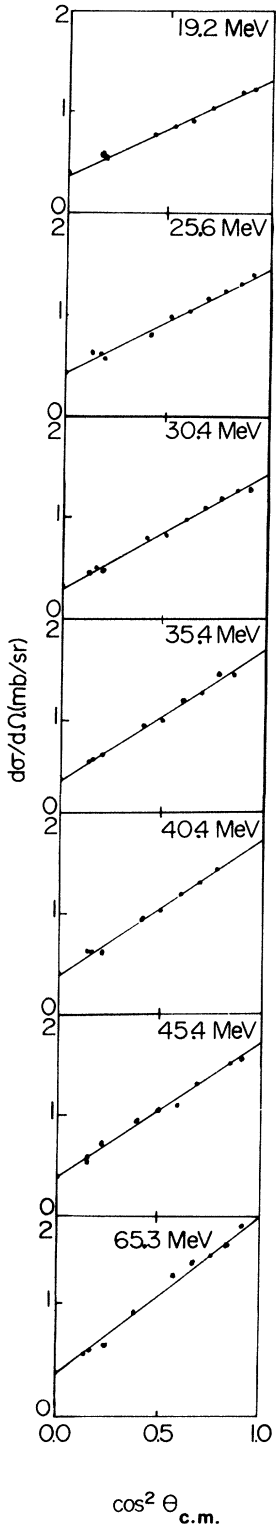

FIG. 2. Differential cross sections determined in this experiment. The fits determined with Eq. (2a) are shown.

The results of these fits are shown in Table II. The fits determined using Eq. (2a) are also shown superimposed on the experimental data in Fig. 2. As may be seen from Table II, the additional $\cos^4\theta$ term produced no significant improvement in the weighted chi-square as the pion energy increased. An improvement would indicate that as the pion energy is increased, higher angular momentum partial waves become important. The presence of the $\cos^4\theta$ term is indicative of d-wave contributions to the scattering process, with some possible contribution from the d-state components in the deuteron ground state wave function.[4]

The total cross sections were determined by

$$\sigma_{\text{tot}} = \int_{2\pi} \frac{d\sigma}{d\Omega}\bigg|_{\text{c.m.}} d\Omega \ ,$$

using the parametrizations of Eq. (2). The total cross sections determined for each energy are given in Table II. The integration over 2π rather than 4π is necessary since the protons emanating from the reaction are indistinguishable. As may be seen, the

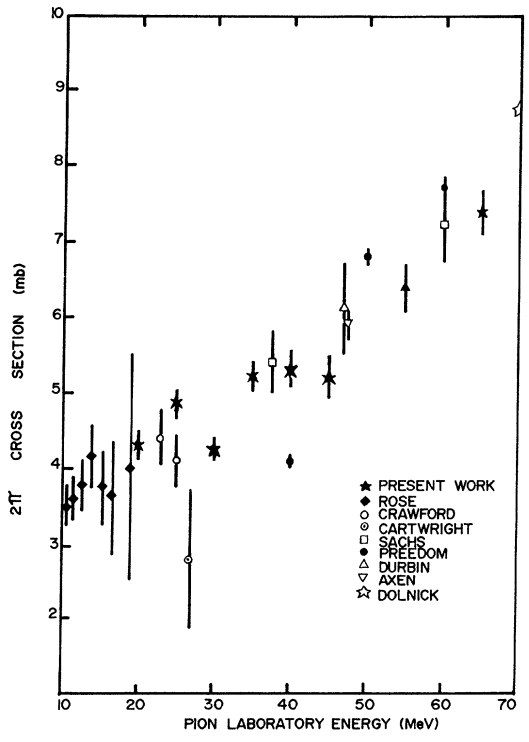

FIG. 3. Total cross sections for the reaction $\pi^+ + d \rightarrow p + p$ determined in this and previous experiments. Note that the integration is over 2π owing to the indistinguishability of the protons emerging from the reaction.

TABLE II. Least squares fit results to measured differential cross sections using the parametrization of Eq. (2). The parameters are all given in units of mb/sr. Uncertainties are enclosed in parentheses. Errors cited for the angular distribution parameters do not include normalization errors. Errors given for the total cross sections are absolute and include normalization and statistical error.

Energy MeV	Eq. (2a) C_0	C_2	χ^2/N	σ (mb)	Eq. (2b) C_0	C_2	C_4	χ^2/N	σ (mb)
20	0.391 (0.010)	0.885 (0.020)	$\frac{6}{10}$	4.309 (0.176)	0.402 (0.012)	0.789 (0.068)	0.114 (0.076)	$\frac{4}{10}$	4.324 (0.177)
25	0.427 (0.011)	1.028 (0.022)	$\frac{29}{11}$	4.837 (0.198)	0.439 (0.014)	0.925 (0.084)	0.119 (0.094)	$\frac{27}{11}$	4.846 (0.199)
30	0.321 (0.007)	1.071 (0.019)	$\frac{30}{11}$	4.260 (0.164)	0.331 (0.009)	0.945 (0.063)	0.165 (0.079)	$\frac{26}{11}$	4.270 (0.166)
35	0.411 (0.009)	1.246 (0.024)	$\frac{14}{10}$	5.191 (0.206)	0.420 (0.012)	1.141 (0.087)	0.142 (0.113)	$\frac{13}{10}$	5.208 (0.207)
40	0.417 (0.008)	1.278 (0.023)	$\frac{21}{9}$	5.298 (0.246)	0.425 (0.011)	1.178 (0.083)	0.146 (0.116)	$\frac{19}{9}$	5.323 (0.248)
45	0.398 (0.009)	1.290 (0.023)	$\frac{29}{10}$	5.201 (0.283)	0.392 (0.010)	1.355 (0.071)	−0.091 (0.094)	$\frac{29}{10}$	5.187 (0.283)
65	0.511 (0.011)	1.997 (0.036)	$\frac{11}{9}$	7.396 (0.303)	0.512 (0.013)	1.984 (0.124)	0.016 (0.047)	$\frac{11}{9}$	7.395 (0.303)

errors are in all cases less than 6% for the parametrization used in (2a). Figure 3 presents the data obtained in this experiment with other data[2,5−20] at pion laboratory energies of 20 to 70 MeV for the total cross section. It appears that the value of the total cross section at 40 MeV which we obtained in a previous work[2] is in error. Specific inquiry into this discrepancy has yielded no explanation for the anomalous result. The value is plotted as given in Ref. 5.

Attempts to understand the reaction process microscopically began with consideration of pion-nucleon rescattering.[21] Work by Riska, Brack, and Weise[22] and Cheon[23] demonstrated the importance of rho meson exchange. Niskanen[24] applied a coupled channels approach to the rho meson exchange and determined both total and differential cross section energy dependences. The Niskanen work also suggested the importance of including $^3F_3$ pp production at energies approaching the πN resonance and above, and indicated that the total and differential cross sections were rather insensitive to the d-state probability of the deuteron, in disagreement with other analyses of the reaction.[25,26]

More recently Chai and Riska[27] (CR) and Maxwell, Weise, and Brack[28] (MWB) used a perturbation theory approach, again including rho meson exchange in their analysis. CR calculated the total and differential cross sections with different models for the pion absorption operator and several sets of deuteron wave functions. They found a high sensitivity to the nucleon-nucleon interactions generating the wave functions used for the deuteron system. Maxwell, Weise, and Brack analyzed the reaction using a model incorporating s-wave rescattering, p-wave and rho-meson rescattering following Δ_{33} excitation, within a recoil corrected impulse approximation calculation. The recoil corrections were found to be significant for pseudovector recoil, and the choice of either the Reid or Paris nucleon-nucleon

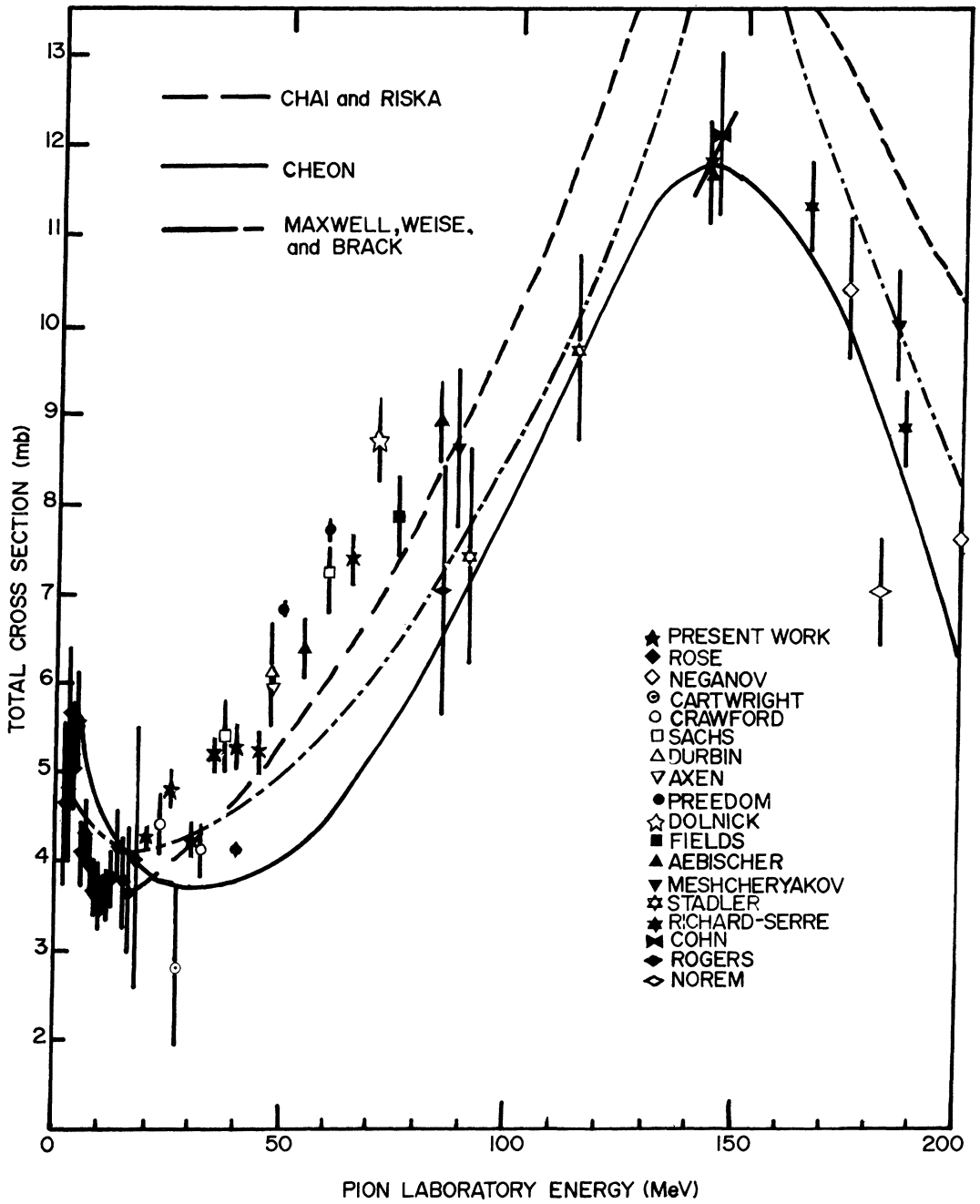

FIG. 4. Calculations of Chai and Riska, Cheon, and Maxwell, Weise, and Brack for the total cross section of the reaction $\pi^+ + d \rightarrow p + p$. The Chai and Riska calculation used the Reid soft-core potential with rho and pion exchange, with meson energy $\omega' = \omega/2$. The Cheon calculation pictured above includes rho exchange. The Maxwell, Weise, and Brack calculation includes pion and rho meson rescattering with pseudovector recoil corrections using the Paris potential.

potential appeared to have little effect on the calculations. MWB have noted that their calculations essentially reproduce the CR calculations when recoil effects are excluded.

The results of the calculations by CR, by Cheon, and by MWB for the total cross section are shown in Fig. 4. The inclusion of pseudovector recoil in the MWB calculations markedly improves the fit to the very low energy data. It is clear that, though the qualitative agreement is quite evident, quantitative agreement still has not been achieved. In general, a trade-off is approached, as noted previously by

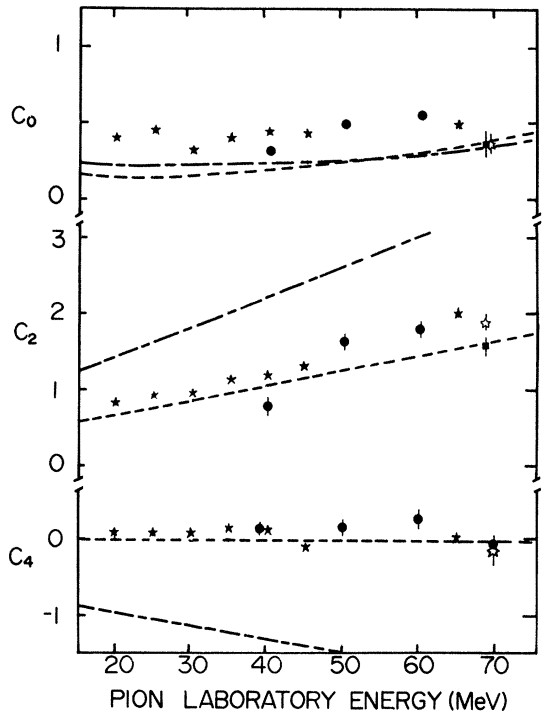

FIG. 5. Calculations of Chai and Riska, and Maxwell, Weise, and Brack for the differential cross section parameters of the reaction $\pi^+ + d \rightarrow p + p$. The Chai and Riska and Maxwell, Weise, and Brack calculations were made as noted in Fig. 4.

MWB, in fitting the total cross section: The magnitude of the total cross section at resonance is fit with a subsequent loss of agreement below resonance, or the below resonance data is fit with a predicted magnitude for the resonance cross section much higher than observed.

The calculations of Chai and Riska and Maxwell, Weise, and Brack for the differential cross section parameters of Eq. (2) are shown in Fig. 5. The inclusion of pseudovector recoil corrections in the MWB calculations drastically deteriorates the overall agreement for these parameters, despite its beneficial effects on the total cross section results. This discrepancy illustrates the importance of the experimental differential cross section measurements to the theoretical understanding of the reaction. The CR calculations may be seen in Fig. 5 to reproduce qualitatively the trends of the data with regard to the angular distributions. Though the calculations may have been improved with the inclusion of additional partial waves, it appears additional details of the reaction process remain to be understood before a quantitative understanding of the properties of the low energy dependences of the total and differential cross section emerges.

IV. CONCLUSION

We have measured the total and differential cross section for the reaction $\pi^+ + d \rightarrow p + p$ over a range of energies below resonance. Our measurements confirm the general trends observed for the reaction in the energy range studied. It appears that current theoretical understanding of the reaction process is insufficient to explain completely the observed total cross sections and angular distributions below resonance.

ACKNOWLEDGMENTS

The authors wish to thank Ray Tipsword of the Virginia Polytechnic Institute and State University and the entire staff at LAMPF for their support and assistance during this experiment. This work was supported by the National Science Foundation (University of South Carolina, Virginia Polytechnic Institute and State University), by the Department of Energy (LASL), and by the Union Carbide Corporation under Contract No. W-7405-eng-26 with the Department of Energy (ORNL).

[1]A. W. Thomas and R. H. Landau, Phys. Rep. 58, 121 (1980).
[2]B. M. Preedom, C. W. Darden, R. D. Edge, T. Marks, M. J. Saltmarsh, K. Gabathuler, E. E. Gross, C. A. Ludemann, P. Y. Bertin, M. Blecher, K. Gotow, J. Alster, R. L. Burman, J. P. Perroud, and R. P. Redwine, Phys. Rev. C 17, 1402 (1978).
[3]B. M. Preedom, M. J. Saltmarsh, C. A. Ludemann, and J. Alster, Nucl. Instrum. Methods 133, 311 (1976).
[4]I. R. Afnan and A. W. Thomas, Phys. Rev. C 10, 109 (1974).
[5]F. S. Crawford and M. L. Stevenson, Phys. Rev. 97, 1305 (1955).
[6]W. F. Cartwright, C. Richman, M. N. Whitehead, and H. A. Wilcox, Phys. Rev. 91, 677 (1953).
[7]A. M. Sachs, H. Winick, and B. A. Wooten, Phys. Rev. 109, 1733 (1958).
[8]D. Axen, G. Duesdieker, L. Felawka, Q. Ingram, and R. Johnson, Nucl. Phys. A256, 387 (1976).
[9]R. Durbin, H. Loar, and J. Steinberger, Phys. Rev. 84, 581 (1951).
[10]D. Aebisher, B. Favier, L. G. Greeniaus, R. Hess, A.

Junod, C. Lechanoine, J.-C. Nikles, D. Rapin, and D. W. Werren, Nucl. Phys. B106, 214 (1976).
[11]C. L. Dolnick, Nucl. Phys. B22, 461 (1971).
[12]T. H. Fields, J. G. Fox, J. A. Kane, R. A. Stallwood, and R. B. Sutton, Phys. Rev. 109, 1704 (1958).
[13]M. G. Meshcheryakov, N. P. Bogacev, and B. S. Neganov, Nuovo Cimento Sup. 3, 120, (1956).
[14]H. L. Stadler, Phys. Rev. 96, 496 (1954).
[15]C. Richard-Serre, W. Hirt, D. F. Measday, E. G. Michaelis, M. J. Saltmarsh, and P. Skarek, Nucl. Phys. B20, 413 (1970).
[16]C. E. Cohn, Phys. Rev. 105, 1582 (1957).
[17]B. S. Neganov and L. B. Parvenov, Zh. Eksp. Teor. Fiz. 34, 767 (1958) [Sov. Phys.—JETP 7, 528 (1958)].
[18]K. C. Rogers and L. M. Lederman, Phys. Rev. 105, 247 (1957).
[19]J. H. Norem, Nucl. Phys. B33, 512 (1971).
[20]C. M. Rose, Phys. Rev. 154, 1305 (1971).
[21]D. S. Koltun, Adv. Nucl. Phys. 3, 71, (1969).
[22]D. O. Riska, M. Brack, and W. Weise, Phys. Lett. 61B, 41 (1972).
[23]I. T. Cheon. Phys. Lett. 90B, 342 (1980).
[24]J. A. Niskanen, Nucl. Phys. A298, 417 (1978).
[25]B. Goplen, W. Gibbs, and E. Lomon, Phys. Rev. Lett. 32, 1012 (1974).
[26]B. M. Preedom, C. W. Darden, R. D. Edge, T. Marks, M. J. Saltmarsh, K. Gabathuler, E. E. Gross, C. A. Ludemann, P. Y. Bertin, M. Blecher, K. Gotow, J. Alster, R. L. Burman, J. P. Perroud, R. P. Redwine, B. Goplen, W. R. Gibbs, and E. L. Lomon, Phys. Lett. 65B, 31 (1976).
[27]J. Chai and D. O. Riska, Nucl. Phys. A338, 349 (1980).
[28]O. V. Maxwell, W. Weise, and M. Brack, Nucl. Phys. A348, 388 (1980).